Research Square

Preprints are preliminary reports that have not undergone peer review. They should not be considered conclusive, used to inform clinical practice, or referenced by the media as validated information.

Identification of a Prognostic Gene Signature Associated with Microenvironment in Acute Myeloid Leukemia

Zhixiang Chen
Xiehe Affiliated Hospital of Fujian Medical University https://orcid.org/0000-0002-2574-2188
Luya Ye
Xiehe Affiliated Hospital of Fujian Medical University
Xuechun Wang
Xiehe Affiliated Hospital of Fujian Medical University
Fuquan Tu
Xiehe Affiliated Hospital of Fujian Medical University
Xuezhen Li
Xiehe Affiliated Hospital of Fujian Medical University
Shao-Yuan Wang (shaoyuanwang@fjmu.edu.cn)
Xiehe Affiliated Hospital of Fujian Medical University https://orcid.org/0000-0001-7428-8682

Primary research

Keywords: Acute myeloid leukemia, Tumor microenvironment, Prognosis, Gene signature, Bioinformatic analysis

Posted Date: October 15th, 2020

DOI: https://doi.org/10.21203/rs.3.rs-91594/v1

License: This work is licensed under a Creative Commons Attribution 4.0 International License.
Read Full License

RESEARCH

Identification of a prognostic gene signature associated with microenvironment in acute myeloid leukemia

Zhixiang Chen[1†] , Luya Ye[1†], Xuechun Wang[1], Fuquan Tu[1], Xuezhen Li[1], Shao-Yuan Wang[12*]

[*]Correspondence:
shaoyuanwang@fjmu.edu.cn
[1]Union Clinical Medical Colleges, Fujian Medical University, Fuzhou, China
[†] These authors have contributed equally to this work

Abstract

Background: Acute myeloid leukemia (AML) is a common hematologic malignancy with poor prognosis. Accumulating reports have indicated that the tumor microenvironment (TME) performs a critical role in the progress of the disease and the clinical outcomes of patients. To date, the role of TME in AML remains clouded due to the complex regulatory mechanisms in it. In this study, We identified key prognostic genes relate to TME in AML and developed a novel gene signature for individualized prognosis assessment.

Methods: The expression profiles of AML samples with clinical information were obtained from the Cancer Genome Atlas (TCGA). The ESTIMATE algorithm was applied to calculate the TME relevant immune and stromal scores. The differentially expressed genes (DEGs) were selected based on the immune and stromal scores. Then, the survival analysis was applied to select prognostic DEGs, and these genes were annotated by functional enrichment analysis. A TME relevant gene signature with predictive capability was constructed by a series of regression analyses and performed well in another cohort from the Gene Expression Omnibus (GEO) database. Moreover, we also developed a nomogram with the integration of the gene signature and clinical indicators to establish an individually quantified risk-scoring system.

Results: In the AML microenvironment, a total of 181 DEGs with prognostic value were clarified. Then a seven-gene (IL1R2, MX1, S100A4, GNGT2, ZSCAN23, PLXNB1 and DPY19L2) signature with robust prediction was identified, and was validated by an independent cohort of AML samples from the GSE71014. Gene set enrichment analysis (GSEA) of genes in the gene signature revealed these genes mainly enriched in the immune and inflammatory related processes. The correlation between the signature-calculated risk scores and the clinical features indicated that patients with high risk scores were accompanied by adverse survival. Finally, a nomogram with clinical utility was constructed.

Conclusion: Our study explored and identified a novel TME relevant seven-gene signature, which could serve as a prognostic indicator for AML. Meanwhile, we also establish a nomogram with clinical significance. These findings might provide new insights into the diagnosis, treatment and prognosis of AML.

Keywords: Acute myeloid leukemia, Tumor microenvironment, Prognosis, Gene signature, Bioinformatic analysis

Introduction

Acute myeloid leukemia (AML) is a hematologic malignancy with severe lethality. It is one of the most common types of blood leukemia in adults[1] and characterized by impaired hematopoiesis and extensive infiltration of immature myeloid hematopoietic cells, especially in the bone marrows[2]. The conventional chemotherapy for the majority of patients with de novo AML includes the "7+3" induction regimen[3, 4], comprising 7 days of cytarabine and 3 days of anthracycline, and the following consolidation chemotherapy or haemopoietic stem cell transplantation (HSCT)[5, 6]. Although many patients received initial remission with this standard strategy, either drug resistance or disease relapse occurred frequently and resulted in final treatment failure.

The treatment effects of AML are influenced by confounding factors. Preceding researches have demonstrated that poor prognosis correlated intensively with advanced age, problematic physical status[7], medical comorbidities[8] and genetic characteristics, which refers to cytogenetics[9-11] and molecular abnormalities[12, 13]. Based on these, targeted therapy specifically against cytogenetics and molecular aberrations are in vigorous clinical development currently[14-16]. Additionally, targeted treatment for tumor microenvironment （TME) has also been proposed and studied for the convincing evidence that the bone marrow microenvironment acts as a vital role in the initiation, progression, and relapse of AML[17, 18].

The TME is defined as a complex regulatory network comprised of tumor cells and surroundings such as immune cells, mesenchymal stem cells, fibroblast cells, endothelial cells, inflammatory cells and extracellular matrix[19, 20]. Among these non-tumor components in the TME, immune cells and stromal cells are two kinds of major participants that work together to impact tumorigenesis, tumor progression, tumor metastasis and therapeutic efficacy[20-22]. The Estimation of Stromal and Immune cells in Malignant Tumour tissues using Expression data (ESTIMATE)[23] method is an algorithm used to calculate immune and stromal scores of tumor samples to predict the infiltration of immune and stromal cells.

Previous studies have widely applied the ESTIMATE algorithm and clarified the meaningful relationship between microenvironment and multiple tumors, including glioblastoma[24], lung adenocarcinoma[25], gastric cancer[26], ovarian cancer[27],etc. The role of TME in AML has been explored and become a hotspot as well. Components in the bone microenvironment have been demonstrated to increase the proliferation of AML cells[28, 29] and

significantly impeded the therapy efficiency[30, 31]. Targeted drugs against the TME of AML have been investigated and displayed good potential for clinical applications[32]. Considering the complex regulatory mechanisms of TME, we therefore believed that elucidating a definite impact of microenvironment on AML is still warranted and might provide new thoughts for the targeted treatment in AML.

In this study, the gene expression profiles and corresponding clinical data of AML samples were obtained from the Cancer Genome Atlas (TCGA)[33] and Gene Expression Omnibus (GEO)[34]. Then the immune and stromal scores for AML cases from TCGA were calculated by ESTIMATE algorithm based on gene expression data. A list of microenvironment relevant differentially expressed genes (DEGs) were screened based on the immune and stromal scores. Several prognostic DEGs were subsequently identified with survival analyses. We further constructed a seven-gene signature with predicting value and validated its robustness using another cohort of AML patients from GEO. Finally, a nomogram with common clinical indexes were generated and revealed favorable predictive performance.

Materials and methods

Database and processing

The gene expression profiles of 137 AML patients with complete clinical information were retrieved from TCGA database (https://portal.gdc.cancer.gov/). The microarray-based gene expression and clinical characteristics of GSE71014[35], including 104 AML patients, were downloaded from GEO database for validation analysis, corresponding to Illumina HumanHT-12 V4.0 expression beadchip GPL10558 platform. The probes in the GSE71014 were converted into the matched gene symbols according to the annotation information in the GPL10558. If multiple probes corresponded to one gene, the mean expression value was defined as a final expression value via the limma[36] package in R language (version 3.6.3).

Identification of DEGs related to AML tumor microenvironment

The immune and stromal scores of 137 AML cases form the TCGA database were assessed via the ESTIMATE algorithm. All AML patients were classified into high and low score groups according to the median immune/stromal scores. The DEGs between low and high score groups were analyzed using limma[36] package with an adjusted P-value <0.05 and |log2 fold change (FC)| >1 as the cutoff criteria. The pheatmap[37] package was used to generate the DEGs associated heatmaps. The results of the intersective high and low DEGs were visualized with VennDiagram package in R.

Kaplan-Meier survival analysis and functional annotation of DEGs

The survival package in R language was used to construct Kaplan-Meier survival curves to identify potential prognostic DEGs. The threshold for survival prognosis signifcance was a P-value<0.05. Both the Kyoto Encyclopedia of Genes and Genomes (KEGG) pathway enrichment analysis and the Gene ontology (GO) categories annotation, including biological processes (BP), molecular functions (MF), and cellular components (CC), were performed among the prognostic DEGs via the clusterProfiler[38] package in R. False discovery rate (FDR) <0.05 was considered as the screening parameter.

Construction of the TME-related gene signature with the prognostic DEGs

The mRNA data from the TCGA cohort were used as the training set. DEGs with predictive capability that determined by the K-M analysis were incorporated into the univariate Cox regression analysis to identify the prognosis relevant genes. We then performed the least absolute shrinkage and selection operator (LASSO) regression with the glmnet package in R to optimize the COX model. The selected genes were later used for multivariate Cox regression analysis to construct a TME-related gene signature. The risk score of individual patient in the gene signature were calculated as follows: risk score = Gene1 expression*β1 + Gene2*β2 +...+ Genen*βn, in which β represents the regression coefficient of each variable.

Verifying the robustness of the gene signature

Transcriptome data of another cohort of AML patients from the GSE71014 were treated as a validation set. The Kaplan-Meier survival analysis was performed to evaluate the difference on survival rates in the high and low risk score groups. The efficacy of the gene signature for predicting the 1-, 3- and 5- year survival events of the training and validation sets were assessed via the time-dependent receiver operating characteristic (ROC) curve by survivalROC package under R environment. Moreover, based on the risk scores of the gene signature, we also introduced the Harrell's index of concordance (C-index) and the calibration plot in the training and validation sets separately to verify the efficacy of the risk signature.

Gene set enrichment analysis

We also explored principal pathways that were up- or down- regulated ranged from different expression levels of genes in the risk model by gene set enrichment analysis[39] (GSEA)(GSEA 4.0.3). The javaGSEA Desktop Application was downloaded from https://www.gsea-msigdb.org/gsea/index.jsp. The enrichment FDR value was identified based on 1,000 permutations, and FDR < 0.05 was considered to be statistical significance.

Deciphering the immune landscape via the CIBERSORT

Patients were separated into high and risk groups based on the seven-gene signature, we then deciphered the unique immune infiltration characteristics in the two groups through the CIBERSORT[40] algorithm.

Establishment of a nomogram

A nomogram was established by integrating the seven-gene signature with the clinical features, including age, gender, cytogenetics, bone marrow blasts, peripheral blood blasts, FAB subtypes and molecular aberrations. Univariate and multivariate Cox regression analyses were carried out to determine the Hazard ratio (HR) of distinct factors.

Results

Correlation of immune and stromal scores with the clinical features and prognosis of AML

A total of 137 AML patients with gene expression data and clinical information were collected from the TCGA database. The patients were diagnosed as AML between 2001 and 2010. 76 (54.97%) patients were males and 61 (45.03%) were females. According to the ESTIMATE algorithm, immune scores were distributed between 1624.55 and 4080.71, while stromal scores ranged from -1810.54 to 338.14.

AML cases were divided into high and low immune or stromal score groups according to the separate median scores to illustrate the potential linkages of clinical parameters with immune and stromal scores. The statistical analyses revealed that high immune scores were more frequently observed in the older AML patients (Figure 1A) or patients with poor or normal cytogenetics. While no obvious connections were observed between the stromal scores and age or cytogenetics features (Fig. 1C, D). Additionally, both of the immune scores and stromal scores showed an apparent association with the FAB morphology (Fig. 1E, F).

We then explored the correlations of overall survival (OS) with immune scores or stromal scores via Kaplan – Meier survival analysis. The results demonstrated that patients with low immune scores showed longer overall survival than patients with high immune scores, although this difference showed no statistical significance (Fig. 1G). As for the stromal groups, no revealing difference was noted in the two groups (Fig. 1H).

Identification of differentially expressed genes (DEGs) related to TME in AML patients

To identify differentially expressed genes (DEGs) associated with TME in AML patients, differential expression analysis was conducted after classifying AML samples into low and high immune/stromal score groups. The cut-off criteria was set as FDR<0.05 and |log2fold change (FC)|>1.0. In all, we identified 885 upregulated genes and 450 downregulated genes in the high

immune score group, compared with the low immune score group (Fig. 2A). Likewise, comparison between the high and low stromal score groups revealed 776 upregulated genes and 369 downregulated genes (Fig. 2B). The DEGs retrived from low and high immune/stromal score groups were presented in the heatmaps respectively (Fig. 2C, D). The intersected genes from both stromal and immune groups were achieved through Venn diagrams for further analysis, including 662 jointly upregulated genes and 196 commonly downregulated genes (Fig. 2E,F). These crossed DEGs were chosen for further discussion.

Survival analysis and functional annotation of crossed DEGs

To determine the prognostic impact of intersective DEGs on OS, we firstly performed Kaplan-Meier survival analysis using the survival package in R. Upon 858 DEGs, 181 DEGs predicted obvious influence on poor prognosis (P-value<0.05). Some selected genes are shown in Figure 3. GO analysis of the 181 DEGs with prognostic value indicated that these genes were enriched in 445 GO terms ($P < 0.05$), including 387 biological processes (BP), 22 cellular components (CC) and 36 molecular functions (MF). The top 10 clustered terms of BP, CC and MF were displayed in Fig. 4A. The result revealed that these genes were mostly enriched in inflammatory relevant response. The enriched KEGG pathways were immune and inflammatory- related as well, such as cytokine－cytokine receptor interaction, NOD－like receptor signaling pathway and B cell receptor signaling pathway (Fig. 4B).

Establishment and validation of a seven-gene signature based on TME analysis

Firstly, we conducted univariate Cox proportional hazard regression analysis among these 181 prognostic DEGs. The resulting 88 genes altogether showed remarkable significance on predictive role ($P<0.05$; Table S1). These genes were subsequently incorporated into the LASSO regression to avoid overfitting problems (Fig. 5A). The multivariate Cox regression analysis were finally constructed with the screened genes from LASSO regression analysis to establish a gene signature with prognostic value (Fig. 5B, Table S2). The risk score for each patient was calculated as follows: risk score = 0.1370 × IL1R2 expression + 0.1693 × MX1 expression + (−0.3866 × ZSCAN23 expression) + (−0.1714 × PLXNB1 expression) + (-0.1046 × DPY19L2 expression) + 0.1189 × S100A4 expression + 0.0238 × GNGT2 expression. Patients were divided into high- and low- risk groups according to the median value of the scores to perform K-M analysis and the result confirmed that patients with high risk scores were more likely to undergo worse clinical outcomes (Fig. 5C). The area under curves (AUCs) of the risk signature for predicting the 1-, 3- and 5-year survival rates were 0.754, 0,743 and 0.772 respectively (Fig. 5D), indicating the

robust ability of the gene signature to distinguish inferior survival events in patients with high risk scores. As the risk score increased, the expression level of IL1R2, MX1, S100A4 and GNGT2 were upregulated while ZSCAN23, PLXNB1 and DPY19L2 were decreased (Fig. 5E). Concomitantly, patients with shorter OS were accumulated in the high risk score group (Fig. 5F).

Another cohort of AML patients from the GSE71014 data was treated as testing group. The AUCs of the ROC curves in the GE71014 for predicting the 1-, 3- and 5- year survival were 0.662, 0.665 and 0.679 respectively (Fig. 5G). Likewise, as the risk score rises, the expression of IL1R2, MX1, S100A4 and GNGT2 were increased while ZSCAN23, PLXNB1 and DPY19L2 declined (Fig. 5H). Meanwhile, patients with high risk scores usually kept pace with worse clinical outcomes (Fig. 5I, J). These results verified the efficient performance of the seven-gene signature in prognosis prediction.

Gene set enrichment analysis of genes in the gene signature

GSEA was implemented to explore the potential mechanisms of the prognostic effects of the TME-related gene signature. KEGG sets analysis revealed that high expression of IL1R2, MX1, S100A4, GNGT2 and low expressed ZSCAN23, PLXNB1 and DPY19L2 mainly participated in the activation of immune and inflammatory related pathways, such as B cell receptor signaling pathway, T cell receptor signaling pathway, TOLL like receptor signaling pathway and chemokine signaling pathway. Moreover, highly expressed IL1R2 was observed to be closely correlated with cancer pathways, including pancreatic cancer and renal cell carcinoma process (Fig. 6). CIBERSOT algorithm was further applied to better understand the discrepancy of the immune landscape between the high and low risk score groups. Interestingly, the result indicated that activated CD4 memory T cells, monocytes presented a higher proportion in the high risk score group, although this dominance revealed no survival influence. As for the low risk score group, there existed elevated plasma cells, CD8 T cells, CD4 memory resting T cells, follicular helper T cells, resting mast cells, activated mast cells and eosinophils (Fig. 7A). And patients with higher proportion of resting mast cells or activated mast cells were considered to deserve better survival (Fig. 7B).

Correlation of gene signature and clinical characteristics

Patients were divided into high and low risk score groups based on the risk model, and the significance test was subsequently applied to investigate the correlation of the gene signature and clinical factors. As demonstrated in the Table1, more of the elderly patients (P=0.000) or patients with normal or poor karyotype (P=0.002) were classified into the high risk score group. Moreover, the

OS of patients in the high risk score group were significantly shorter than that of patients in the low risk group, whether for the median OS or range consideration (P=0.000). We were interested to find that patients with low risk score were observed with higher bone marrow blasts (P=0.003). No significance differences in the gender distribution, FAB monocyte, peripheral blasts percentage and the molecular abnormalities were identified between the low and high risk groups.

Nomogram deduction by integrating gene expression with clinical indicators

We further constructed a nomogram via the Cox regression analyses for clinical utility. This nomogram was comprised of the seven gene transcriptome and several clinical variables, including age, gender, cytogenetics, bone marrow blasts, peripheral blasts, FAB subtypes and molecular aberrations (Fig. 8A). Both the univariate and multivariate Cox regression models revealed that the the seven-gene signature could act as a powerful biomarker for predictive application (Fig. 8B, C). The C-index of the nomogram was 0.755 (95% CI; 0.7040 – 0.8060). The area under the curves (AUCs) of the 1-, 3- and 5-year OS predictions for the constructed nomogram were 0.807, 0.843 and 0.904 (Fig. 8 D, E, F). Moreover, the calibration curves of this nomogram were plotted and indicated that the nomogram could precisely predict the 1-, 3 - and 5- year survival events (Fig. 8 G, H, I).

DISCUSSION

Accumulating evidence indicates that abnormal actions in the tumor microenvironment are essential mechanisms that impact the development, progression and relapse of AML[20-22]. Thus, drugs that specifically target the TME have been studied recently and some of which have already been investigated to improve the clinical efficacy of AML patients[32]. In this study, we aimed to identify the prognostic biomarkers of TME in AML to further enrich the insights of target therapy and provide feasible strategy for clinical practice by analyzing the transcriptome and clinical data retrieved from the TCGA and GEO databases.

For 137 AML patients in the TCGA database, the individual immune and stromal scores were calculated by the ESTIMATE algorithm. The result showed that high immune scores were associated with elder AML patients and patients characterized by poor or normal karyotype apparently. Moreover, the closely correlation between the immune/stromal scores and the FAB morphology were clarified. Kaplan-Meier survival curves indicated that higher immune scores usually portended unfavorable clinical outcomes. These results are the same as previous studies[41, 42].

We then stratified the 137 patients into high and low groups according to the immune or stromal scores. The crossed DEGs of the TME were identified via intersecting the DEGs derived from high versus low immune score groups and high versus low stromal score groups separately. We subsequently investigated the prognostic role of the commonly DGEs with Kaplan-Meier survival analysis and 181 DEGs altogether were determined. GO analysis revealed that these prognostic DEGs primarily enriched in inflammatory relevant response. Likewise, the enriched KEGG pathways were immune and inflammatory-related as well, such as cytokine – cytokine receptor interaction, NOD – like receptor signaling pathway and B cell receptor signaling pathway. ALL of these pathways have been reported to participated in the development of blood tumors[43-46]. Moreover, the B cell receptor signaling pathway has already been investigated in depth and considered as a promising therapeutic target for hematological malignancy, including CLL[47], ALL[48], AML[49], etc. .

We also administered LASSO Cox regression model together with univariate and multivariate Cox regression analyses in the prognostic DEGs to construct a gene signature with predictive role. The gene signature consisted of seven genes, they are IL1R2, MX1, S100A4, GNGT2, ZSCAN23, PLXNB1 and DPY19L2. The risk score of each patient was calculated later. As the risk scores increased, the expression of IL1R2, MX1, S100A4 and GNGT2 were upregulated while ZSCAN23, PLXNB1 and DPY19L2 were downregulated. Patients with high risk scores were tend to suffer from significantly worse clinical outcomes. In chorus, the ROC analysis reflected a satisfactory accuracy of the risk signature (AUC = 0.754, 0,743 and 0.772 for predicting the 1-, 3- and 5- year survival rates respectively). To prove the efficacy of the seven-gene signature for predictive use, an independent cohort of AML patients from the GSE71014 dataset was assessed for validation purpose. The conclusions kept consistent with the TCGA results, indicating the robustness and stability of the prognostic model.

Previous study have demonstrated that overexpressed S100A4 was highly prevalent in AML and caused disappointing clinical events[50, 51]. Although several genes among these still retained limited evidence regarding the impacts on AML, the correlation between these genes and other tumors or immune response are experiencing a universal investigation. High IL1R2 expression was observed in the Hodgkin lymphoma (HL) and was deemed as a novel risk factor in HL[52]. Additionally, previous study have already pinpointed the contribution of IL1R2 in breast tumorigenesis, demonstrating its potential as a drug target[53]. MX1, namely MxA, a kind of GTPase protein that accumulates in the cytoplasm in response to interferon alpha/beta stimulation, displaying antiviral

activity against several RNA viruses[54]. MX1 was considered to involve in the tumor invasion and lymphatic metastasis in colorectal carcinoma[55]. GNGT2 has been shown to promote the proliferation of esophageal cancer cells[56]. In our study, the role of PLXNB1 has been viewed as a protective factor. Conversely, one research revealed that the crosstalk operated by the CD100+ leukemic cells and PLXNB1 might facilitate the proliferation and survival of chronic lymphocytic leukemia cells[57]. The controversial performance might be brought about due to the unique features in the different disorders, and explicit exploration is needed in the future.

As expected, GSEA indicated that high expression of IL1R2, MX1, S100A4, GNGT2 and low expressed ZSCAN23, PLXNB1 and DPY19L2 mainly activate the immune and inflammatory related pathways, such as B cell receptor signaling pathway, T cell receptor signaling pathway, TOLL like receptor signaling pathway and chemokine signaling pathway. Preceding researches have elucidated the significant role of these pathways in regulating leukemia cells under aberrant activation[47, 48, 58-60]. All in all, these genes may influence the development of AML via these pathways. CIBERSOT algorithm revealed the distinct distribution of 22 immune cells between the high and low risk score groups. An elevated proportion of resting mast cells or activated mast cells presented in the low risk score groups and signaled a good prognosis.

We finally established a nomogram by integrating the seven-gene signature with clinical traits for the purpose of predicting individual clinical outcomes. The efficient performance of the nomogram was validated with a C-index of 0.755, the ROC curves and the calibration plots.

In this study, we firstly explored and identified the TME-related DEGs in AML patients from the TCGA database. Then we investigated the prognostic role of these DEGs. A gene signature with predictive value was later constructed and its efficacy and accuracy was validated by another cohort from the GEO datasets. We finally established a nomogram combing the seven-gene signature with clinical features in favor of supplying diagnostic and prognostic relevant information effectively. Our results suggested that genes involved in the signature showed significant correlation with clinical outcomes of AML and displayed robust potential as biomarkers for targeted therapy in AML.

Conclusion

In conclusion, we explored the prognostic value and pathogenic mechanisms of microenvironment in AML via the transcriptome analysis. A seven-gene signature with precise predictive capability, including IL1R2, MX1, S100A4, GNGT2, ZSCAN23, PLXNB1 and DPY19L2, was established and was combined with

common clinical indexes to provide guidelines for individually clinical decisions. Our work might also refined the insights of AML microenvironment theoretically.

Acknowledgements
The authors would like to express our sincere thanks for sharing the data from The Cancer Genome Atlas (TCGA) database and Gene Expression Omnibus (GEO).

Funding
The research was funded by the National Natural Science Foundation of China (Grant/Award Number: 81770163, 81270609, 81470008, 81500139); Fujian Province Health Education Joint Research Project (Grant/Award Number: WKJ-2016-2-07); Special Funding of Fujian Provincial Department of Finance (Grant/Award Number: Min2017-655); Construction Project of Fujian Medical Center of Hematology (Grant/Award Number: Min201704); The National and Fujian Provincial Key Clinical Specialty Discipline Construction Program, P.R.C (Grant/Award Number:2011-1006, 2012-149).

Abbreviations
AML:Acute myeloid leukemia; OS:overall survival; TME:tumor microenvironment; TCGA:the Cancer Genome Atlas; GEO:Gene Expression Omnibus; DEGs:differentially expressed genes; GSEA:Gene set enrichment analysis; HSCT:haemopoietic stem cell transplantation; KEGG:the Kyoto Encyclopedia of Genes and Genomes; ESTIMATE:The Estimation of Stromal and Immune cells in Malignant Tumour tissues using Expression data; GO:Gene ontology; BP:biological processes; MF:molecular functions; CC:cellular components; FDR:False discovery rate; LASSO regression:least absolute shrinkage and selection operator regression; C-index:index of concordance; ROC:receiver operating characteristic; AUCs:The area under curves; HL:Hodgkin lymphoma. CLL:chronic lymphocytic leukemia； ALL:acute lymphoblastic leukemia； IL1R2：Interleukin-1 Receptor Type II; MX1：MX Dynamin Like GTPase 1; S100A4：S100 Calcium Binding Protein A4; GNGT2：G Protein Subunit Gamma Transducin 2; ZSCAN23：Zinc Finger And SCAN Domain Containing 23; PLXNB1:Plexin B1; DPY19L2：Dpy-19-Like Protein 2.

Acknowledgement
Not applicable.

Ethics approval and consent to participate
Not applicable.

Competing interests
The authors declare that they have no competing interests.

Consent for publication
Not applicable.

Authors' contributions
SW and ZC: study design. ZC: data analysis, figures preparation and wrote the manuscript. LY: data analysis and wrote the manuscript. XW, FT and XL were responsible for the manuscript revision. All authors read and approved the final manuscript.

Author details
[1]Union Clinical Medical Colleges, Fujian Medical University, Fuzhou, China. [2]Department of Hematology, Fujian Institute of Hematology, Fujian Provincial Key Laboratory on Hematology, Fujian Medical University Union Hospital, Fuzhou, China

References
1. Tallman MS, Wang ES, Altman JK, Appelbaum FR, Bhatt VR, Bixby D, Coutre SE, De Lima M, Fathi AT, Fiorella M et al: Acute Myeloid Leukemia, Version 3.2019, NCCN Clinical Practice Guidelines in Oncology. J Natl Compr Canc Netw 2019, 17(6):721-749.
2. Estey E, Döhner H: Acute myeloid leukaemia. Lancet 2006, 368(9550):1894-1907.
3.. Rai KR, Holland JF, Glidewell OJ, Weinberg V, Brunner K, Obrecht JP, Preisler HD, Nawabi IW, Prager D, Carey RW et al: Treatment of acute myelocytic leukemia: a study by cancer and leukemia group B. Blood 1981, 58(6):1203-1212.
4. Yates J, Glidewell O, Wiernik P, Cooper MR, Steinberg D, Dosik H, Levy R, Hoagland C, Henry P, Gottlieb A et al: Cytosine arabinoside with daunorubicin or adriamycin for therapy of acute myelocytic leukemia: a CALGB study. Blood 1982, 60(2):454-462.
5. Short NJ, Konopleva M, Kadia TM, Borthakur G, Ravandi F, DiNardo CD, Daver N: Advances in the Treatment of Acute Myeloid Leukemia: New Drugs and New Challenges. Cancer Discov 2020, 10(4):506-525.
6. Döhner H, Weisdorf DJ, Bloomfield CD: Acute Myeloid Leukemia. N Engl J Med 2015, 373(12):1136-1152.
7. Kantarjian H, O'Brien S, Cortes J, Giles F, Faderl S, Jabbour E, Garcia-Manero G, Wierda W, Pierce S, Shan J et al: Results of intensive chemotherapy in 998 patients age 65 years or older with acute myeloid leukemia or high-risk myelodysplastic syndrome: predictive prognostic models for outcome. Cancer 2006, 106(5):1090-1098.
8. Djunic I, Virijevic M, Novkovic A, Djurasinovic V, Colovic N, Vidovic A, Suvajdzic-Vukovic N, Tomin D: Pretreatment risk factors and importance of comorbidity for overall survival, complete remission, and early death in patients with acute myeloid leukemia. Hematology (Amsterdam, Netherlands) 2012, 17(2):53-58.
9. Mrózek K, Heerema NA, Bloomfield CD: Cytogenetics in acute leukemia. Blood Rev 2004, 18(2):115-136.
10. Fröhling S, Schlenk RF, Kayser S, Morhardt M, Benner A, Döhner K, Döhner H: Cytogenetics and age are major determinants of outcome in intensively treated acute myeloid leukemia patients older than 60 years: results from AMLSG trial AML HD98-B. Blood 2006, 108(10):3280-3288.
11. Grimwade D: Impact of Cytogenetics on Clinical Outcome in AML. In.; 2007: 177-192.
12. Papaemmanuil E, Gerstung M, Bullinger L, Gaidzik VI, Paschka P, Roberts ND, Potter NE, Heuser M, Thol F, Bolli N et al: Genomic Classification and Prognosis in Acute Myeloid Leukemia. N Engl J Med 2016, 374(23):2209-2221.
13. Jongen-Lavrencic M, Grob T, Hanekamp D, Kavelaars FG, Al Hinai A, Zeilemaker A, Erpelinck-Verschueren CAJ, Gradowska PL, Meijer R, Cloos J et al: Molecular Minimal Residual Disease in Acute Myeloid Leukemia. N Engl J Med 2018, 378(13):1189-1199.
14. DiNardo CD, Pratz KW, Letai A, Jonas BA, Wei AH, Thirman M, Arellano M, Frattini MG, Kantarjian H, Popovic R et al: Safety and preliminary efficacy of venetoclax with decitabine or azacitidine in elderly patients with previously untreated acute myeloid leukaemia: a non-randomised, open-label, phase 1b study. Lancet Oncol 2018, 19(2):216-228.
15. DiNardo CD, Stein EM, de Botton S, Roboz GJ, Altman JK, Mims AS, Swords R, Collins RH, Mannis

GN, Pollyea DA et al: Durable Remissions with Ivosidenib in IDH1-Mutated Relapsed or Refractory AML. N Engl J Med 2018, 378(25):2386-2398.
16. Perl AE, Martinelli G, Cortes JE, Neubauer A, Berman E, Paolini S, Montesinos P, Baer MR, Larson RA, Ustun C et al: Gilteritinib or Chemotherapy for Relapsed or Refractory -Mutated AML. N Engl J Med 2019, 381(18):1728-1740.
17. Allan DS, De Lisio M: Reversing pathological remodelling of the bone marrow microenvironment in acute myeloid leukemia. Stem Cell Investig 2018, 5:29.
18. Miller LH, Qu C-K, Pauly M: Germline mutations in the bone marrow microenvironment and dysregulated hematopoiesis. Exp Hematol 2018, 66:17-26.
19. Barcellos-Hoff MH, Lyden D, Wang TC: The evolution of the cancer niche during multistage carcinogenesis. Nat Rev Cancer 2013, 13(7):511-518.
20. Junttila MR, de Sauvage FJ: Influence of tumour micro-environment heterogeneity on therapeutic response. Nature 2013, 501(7467):346-354.
21. Turley SJ, Cremasco V, Astarita JL: Immunological hallmarks of stromal cells in the tumour microenvironment. Nat Rev Immunol 2015, 15(11):669-682.
22. Wu T, Dai Y: Tumor microenvironment and therapeutic response. Cancer letters 2017, 387:61-68.
23. Yoshihara K, Shahmoradgoli M, Martínez E, Vegesna R, Kim H, Torres-Garcia W, Treviño V, Shen H, Laird PW, Levine DA et al: Inferring tumour purity and stromal and immune cell admixture from expression data. Nat Commun 2013, 4:2612.
24. Jia D, Li S, Li D, Xue H, Yang D, Liu Y: Mining TCGA database for genes of prognostic value in glioblastoma microenvironment. Aging (Albany NY) 2018, 10(4):592-605.
25. Qu Y, Cheng B, Shao N, Jia Y, Song Q, Tan B, Wang J: Prognostic value of immune-related genes in the tumor microenvironment of lung adenocarcinoma and lung squamous cell carcinoma. Aging (Albany NY) 2020, 12(6):4757-4777.
26. Refolo MG, Lotesoriere C, Messa C, Caruso MG, D'Alessandro R: Integrated immune gene expression signature and molecular classification in gastric cancer: New insights. J Leukoc Biol 2020.
27. Ding Q, Dong S, Wang R, Zhang K, Wang H, Zhou X, Wang J, Wong K, Long Y, Zhu S et al: A nine-gene signature related to tumor microenvironment predicts overall survival with ovarian cancer. Aging (Albany NY) 2020, 12(6):4879-4895.
28. Konopleva M, Konoplev S, Hu W, Zaritskey AY, Afanasiev BV, Andreeff M: Stromal cells prevent apoptosis of AML cells by up-regulation of anti-apoptotic proteins. Leukemia 2002, 16(9):1713-1724.
29. Spoo AC, Lübbert M, Wierda WG, Burger JA: CXCR4 is a prognostic marker in acute myelogenous leukemia. Blood 2007, 109(2):786-791.
30. Matsunaga T, Takemoto N, Sato T, Takimoto R, Tanaka I, Fujimi A, Akiyama T, Kuroda H, Kawano Y, Kobune M et al: Interaction between leukemic-cell VLA-4 and stromal fibronectin is a decisive factor for minimal residual disease of acute myelogenous leukemia. Nat Med 2003, 9(9):1158-1165.
31. Mony U, Jawad M, Seedhouse C, Russell N, Pallis M: Resistance to FLT3 inhibition in an in vitro model of primary AML cells with a stem cell phenotype in a defined microenvironment. Leukemia 2008, 22(7):1395-1401.
32. Nervi B, Ramirez P, Rettig MP, Uy GL, Holt MS, Ritchey JK, Prior JL, Piwnica-Worms D, Bridger G, Ley TJ et al: Chemosensitization of acute myeloid leukemia (AML) following mobilization by the CXCR4 antagonist AMD3100. Blood 2009, 113(24):6206-6214.
33. Weinstein JN, Collisson EA, Mills GB, Shaw KRM, Ozenberger BA, Ellrott K, Shmulevich I, Sander C, Stuart JM: The Cancer Genome Atlas Pan-Cancer analysis project. Nat Genet 2013, 45(10):1113-1120.
34. Barrett T, Wilhite SE, Ledoux P, Evangelista C, Kim IF, Tomashevsky M, Marshall KA, Phillippy KH, Sherman PM, Holko M et al: NCBI GEO: archive for functional genomics data sets--update. Nucleic Acids Res 2013, 41(Database issue):D991-D995.
35. Chuang M-K, Chiu Y-C, Chou W-C, Hou H-A, Tseng M-H, Kuo Y-Y, Chen Y, Chuang EY, Tien H-F: An mRNA expression signature for prognostication in de novo acute myeloid leukemia patients with normal karyotype. Oncotarget 2015, 6(36):39098-39110.
36. Ritchie ME, Phipson B, Wu D, Hu Y, Law CW, Shi W, Smyth GK: limma powers differential expression analyses for RNA-sequencing and microarray studies. Nucleic Acids Res 2015, 43(7):e47.
37. Gu Z, Eils R, Schlesner M: Complex heatmaps reveal patterns and correlations in multidimensional genomic data. Bioinformatics 2016, 32(18):2847-2849.
38. Yu G, Wang L-G, Han Y, He Q-Y: clusterProfiler: an R package for comparing biological themes among gene clusters. OMICS 2012, 16(5):284-287.
39. Subramanian A, Tamayo P, Mootha VK, Mukherjee S, Ebert BL, Gillette MA, Paulovich A, Pomeroy SL, Golub TR, Lander ES et al: Gene set enrichment analysis: a knowledge-based approach for interpreting genome-wide expression profiles. Proc Natl Acad Sci USA 2005, 102(43):15545-15550.
40. Newman AM, Liu CL, Green MR, Gentles AJ, Feng W, Xu Y, Hoang CD, Diehn M, Alizadeh AA: Robust enumeration of cell subsets from tissue expression profiles. Nat Methods 2015, 12(5):453-457.
41. Huang S, Zhang B, Fan W, Zhao Q, Yang L, Xin W, Fu D: Identification of prognostic genes in the acute myeloid leukemia microenvironment. Aging (Albany NY) 2019, 11(22):10557-10580.
42. Yan H, Qu J, Cao W, Liu Y, Zheng G, Zhang E, Cai Z: Identification of prognostic genes in the acute myeloid leukemia immune microenvironment based on TCGA data analysis. Cancer Immunol Immunother 2019, 68(12):1971-1978.
43. Herishanu Y, Pérez-Galán P, Liu D, Biancotto A, Pittaluga S, Vire B, Gibellini F, Njuguna N, Lee E, Stennett L et al: The lymph node microenvironment promotes B-cell receptor signaling, NF-kappaB activation, and tumor proliferation in chronic lymphocytic leukemia. Blood 2011, 117(2):563-574.
44. Mirji G, Bhat J, Kode J, Banavali S, Sengar M, Khadke P, Sait O, Chiplunkar S: Risk stratification of T-cell Acute Lymphoblastic Leukemia patients based on gene expression, mutations and copy number variation. Leuk Res 2016, 45:33-39.
45. Niu P, Yao B, Wei L, Zhu H, Fang C, Zhao Y: Construction of prognostic risk prediction model based on high-throughput sequencing expression profile data in childhood acute myeloid leukemia. Blood Cells Mol Dis 2019, 77:43-50.
46. Buteyn NJ, Santhanam R, Merchand-Reyes G, Murugesan RA, Dettorre GM, Byrd JC, Sarkar A, Vasu S, Mundy-Bosse BL, Butchar JP et al: Activation of the Intracellular Pattern Recognition Receptor NOD2 Promotes Acute Myeloid Leukemia (AML) Cell Apoptosis and Provides a Survival Advantage in an Animal Model of AML. Journal of immunology (Baltimore, Md : 1950) 2020, 204(7):1988-1997.
47. Woyach JA, Johnson AJ, Byrd JC: The B-cell receptor signaling pathway as a therapeutic target in CLL. Blood 2012, 120(6):1175-1184.
48. Grupp SA, Kalos M, Barrett D, Aplenc R, Porter DL, Rheingold SR, Teachey DT, Chew A, Hauck B, Wright JF et al: Chimeric antigen receptor-modified T cells for acute lymphoid leukemia. N Engl J Med 2013, 368(16):1509-1518.
49. Walker AR, Bhatnagar B, Marcondes AMQ, DiPaolo J, Vasu S, Mims AS, Klisovic RB, Walsh KJ, Canning R, Behbehani GK et al: Interim Results of a Phase 1b/2 Study of Entospletinib (GS-9973) Monotherapy and in Combination with Chemotherapy in Patients with Acute Myeloid Leukemia. Blood 2016, 128(22):2831-2831.
50. Dong X, Fang Z, Yu M, Zhang L, Xiao R, Li X, Pan G, Liu J: Knockdown of Long Noncoding RNA HOXA-AS2 Suppresses Chemoresistance of Acute Myeloid Leukemia via the miR-520c-3p/S100A4 Axis. Cell Physiol Biochem 2018, 51(2):886-896.
51. Alanazi B, Munje CR, Rastogi N, Williamson AJK, Taylor S, Hole PS, Hodges M, Doyle M, Baker S,

Gilkes AF et al: Integrated nuclear proteomics and transcriptomics identifies S100A4 as a therapeutic target in acute myeloid leukemia. Leukemia 2020, 34(2):427-440.
52. Ma Y, Visser L, Roelofsen H, de Vries M, Diepstra A, van Imhoff G, van der Wal T, Luinge M, Alvarez-Llamas G, Vos H et al: Proteomics analysis of Hodgkin lymphoma: identification of new players involved in the cross-talk between HRS cells and infiltrating lymphocytes. Blood 2008, 111(4):2339-2346.
53. Zhang L, Qiang J, Yang X, Wang D, Rehman AU, He X, Chen W, Sheng D, Zhou L, Jiang Y-Z et al: IL1R2 Blockade Suppresses Breast Tumorigenesis and Progression by Impairing USP15-Dependent BMI1 Stability. Adv Sci (Weinh) 2020, 7(1):1901728.
54. Gordien E, Rosmorduc O, Peltekian C, Garreau F, Bréchot C, Kremsdorf D: Inhibition of hepatitis B virus replication by the interferon-inducible MxA protein. J Virol 2001, 75(6):2684-2691.
55. Croner RS, Stürzl M, Rau TT, Metodieva G, Geppert CI, Naschberger E, Lausen B, Metodiev MV: Quantitative proteome profiling of lymph node-positive vs. -negative colorectal carcinomas pinpoints MX1 as a marker for lymph node metastasis. Int J Cancer 2014, 135(12):2878-2886.
56. Liu G-M, Ji X, Lu T-C, Duan L-W, Jia W-Y, Liu Y, Sun M-L, Luo Y-G: Comprehensive multi-omics analysis identified core molecular processes in esophageal cancer and revealed GNGT2 as a potential prognostic marker. World J Gastroenterol 2019, 25(48):6890-6901.
57. Granziero L, Circosta P, Scielzo C, Frisaldi E, Stella S, Geuna M, Giordano S, Ghia P, Caligaris-Cappio F: CD100/Plexin-B1 interactions sustain proliferation and survival of normal and leukemic CD5+ B lymphocytes. Blood 2003, 101(5):1962-1969.
58. Majeti R, Becker MW, Tian Q, Lee T-LM, Yan X, Liu R, Chiang J-H, Hood L, Clarke MF, Weissman IL: Dysregulated gene expression networks in human acute myelogenous leukemia stem cells. Proc Natl Acad Sci USA 2009, 106(9):3396-3401.
59. Liang X, Moseman EA, Farrar MA, Bachanova V, Weisdorf DJ, Blazar BR, Chen W: Toll-like receptor 9 signaling by CpG-B oligodeoxynucleotides induces an apoptotic pathway in human chronic lymphocytic leukemia B cells. Blood 2010, 115(24):5041-5052.
60. Shi Y, Tomic J, Wen F, Shaha S, Bahlo A, Harrison R, Dennis JW, Williams R, Gross BJ, Walker S et al: Aberrant O-GlcNAcylation characterizes chronic lymphocytic leukemia. Leukemia 2010, 24(9):1588-1598.

Figure 1 The relationship of immune/stromal scores with clinical parameters and overall survival. Distribution of immune scores within different groups classified by age (A), cytogenetics (B), FAB morphology (E). Distribution of stromal scores within different groups classified by age (C), cytogenetics (D), FAB morphology (F). G, Comparison of overall survival between high and low immune scores groups. H, Comparison of overall survival between high and low stromal scores groups. FAB morphology, French American British (FAB) morphological classification

Figure 2 Identification of TME related DEGs in AML patients. The volcano diagrams about differentially expressed mRNAs in high immune score group (A) and low immune score group (B). Heatmaps of DEGs clustering in immune score group (C) and stromal score group (D), respectively. E, Intersection Venn diagram of significant high expression genes of immune score group and stromal score group. F, Intersection Venn diagram of significant low expression genes of immune score group and stromal score group. DEGs, differentially expressed genes; AML, acute myeloid leukemia

Figure 3 Kaplan-Meier curves of OS for crossed DEGs. DEGs, differentially expressed genes; AML, acute myeloid leukemia; OS, overall survival

Figure 4 Functional enrichment analysis of crossed DEGs with prognostic indication. A, The results of GO biological process enrichment, cellular component enrichment and molecular function enrichment. B, The result of KEGG pathways analysis of crossed DEGs. DEGs, differentially expressed genes; GO, Gene Ontology; KEGG, Kyoto Encyclopedia of Genes and Genomes

Figure 5 Establishment of a seven-gene signature in the TCGA database and verified with GSE71014 data. A, LASSO coefficient profiles of genes screened from univariate Cox regression analysis (left), The partial likelihood deviance plot selected the best parameters in LASSO model (right). B, Seven genes (IL1R2, MX1,ZSCAN23, PLXNB1 ,DPY19L2,S100A4 and GNGT2) were selected for constructing a gene signature using multivariate Cox regression model. C, Kaplan-Meier survival curves showed the prognostic value of the risk signature between low-risk group and high-risk group in the TCGA database. D, The AUCs of the gene signature for predicting the 1-, 3- and 5-year survival rates in the TCGA database. E, F, The seven genes expression profiles, the risk scores distribution and patients' survival status in the TCGA database. G, The AUCs of the gene signature for predicting the 1-, 3- and 5-year survival rates in the GSE71014 dataset. H, I, The seven genes expression profiles, the risk scores distribution and patients' survival status in the GSE71014 dataset. J, Kaplan-Meier survival curves showed the prognostic value of the risk signature between low-risk group and high-risk group in the GSE71014 dataset. TME, tumor microenvironment; TCGA, The Cancer Genome Atlas; AUC, the area under curves

Figure 6 Results of gene set enrichment analysis of genes in the gene signature

Figure 7 Violin plot of immune infiltration signatures in the high and low risk score groups (A) . Kaplan-Meier survival curves showed the prognostic value of activated mast cells(left)

and resting mast cells(right) between low proportion and high proportion(B).

Figure 8 Construction of a nomogram for predicting 1−, 3− and 5−y survival of AML. A, A nomogram for predicting 1−, 3− and 5−y survival rates of AML patients. The univariate(B) and multivariate Cox regression models(C) evaluated the contribution of each variable to AML survival. The AUCs assessed the efficiency of the nomogram for predicting 1− (D), 3− (E) and 5−y (F) survival. Calibration curves showed the probability of 1− (G), 3− (H) and 5−y survival (I) between the prediction and the observation. AML, acute myeloid leukemia; AUC, the area under curves

Table 1 Relationship between risk scores and clinical characteristics.

Supplement Table S1 A total of 88 genes showed predictive value via univariate Cox proportional hazard regression analysis.

Supplement Table S2 The coefficents of genes in the prognostic gene signature.

Figures

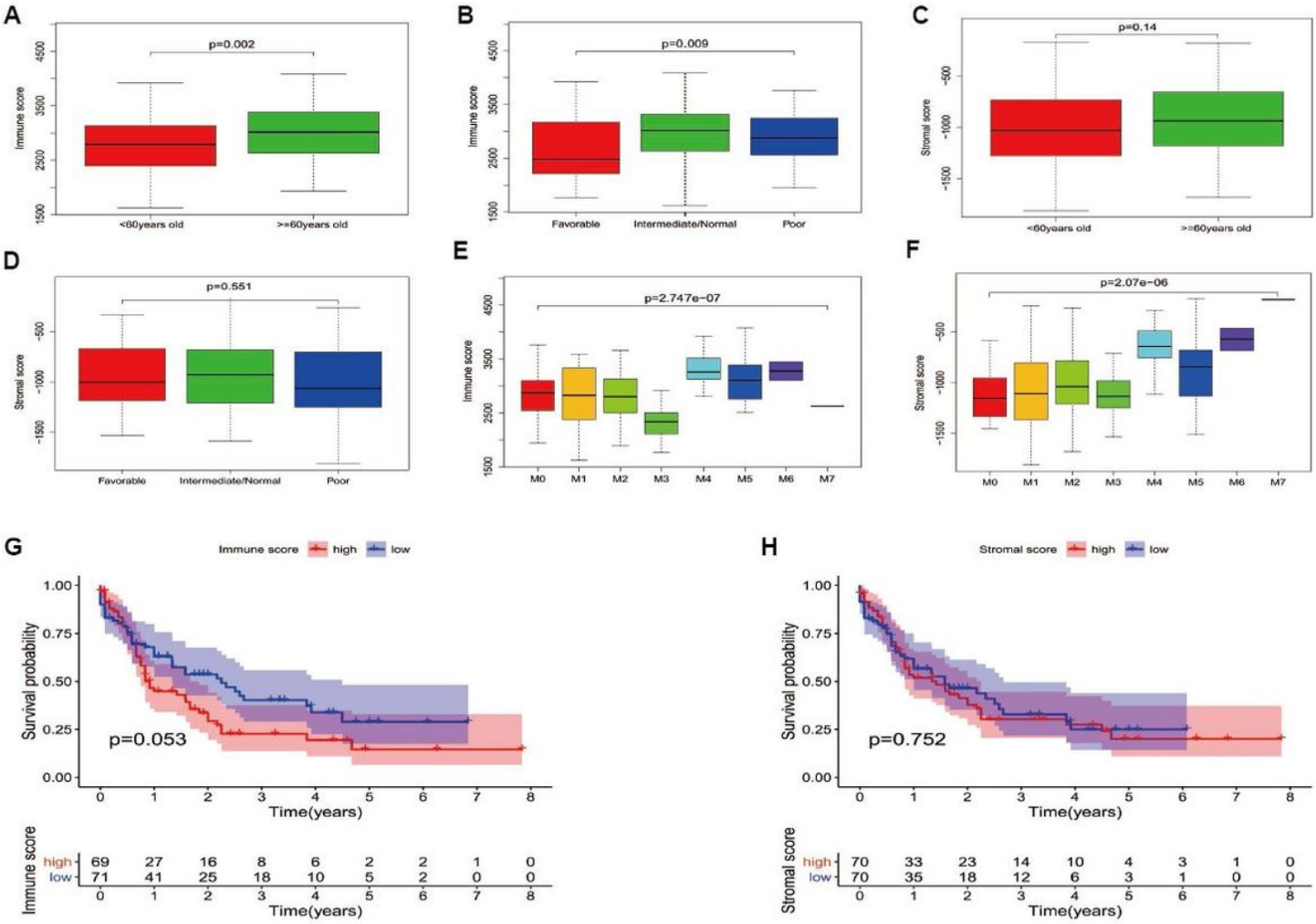

Figure 1

The relationship of immune/stromal scores with clinical parameters and overall survival. Distribution of immune scores within different groups classified by age (A), cytogenetics (B), FAB morphology (E). Distribution of stromal scores within different groups classified by age (C), cytogenetics (D), FAB morphology (F). G, Comparison of overall survival between high and low immune scores groups. H, Comparison of overall survival between high and low stromal scores groups. FAB morphology, French American British (FAB) morphological classification

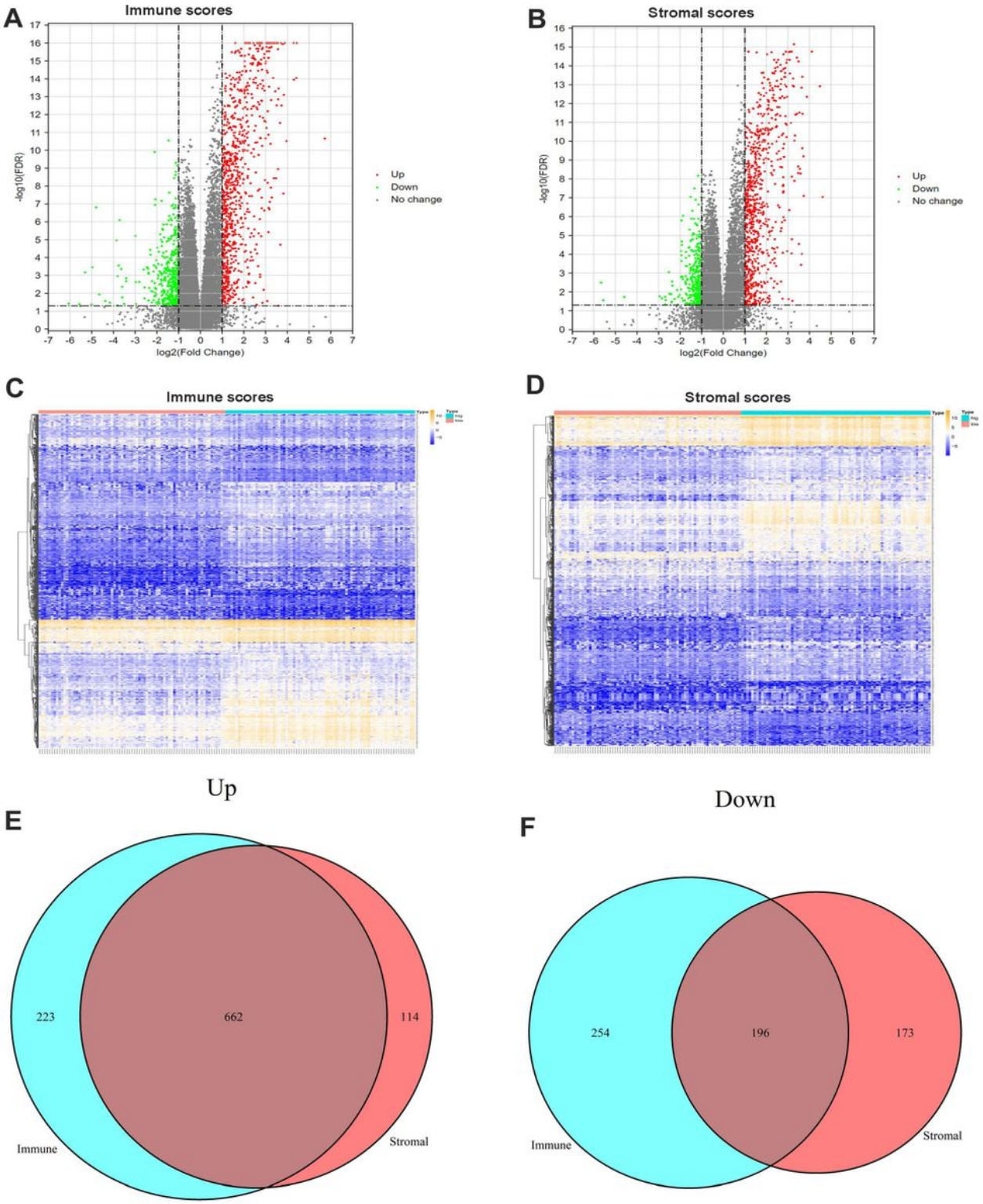

Figure 2

Identification of TME related DEGs in AML patients. The volcano diagrams about differentially expressed mRNAs in high immune score group (A) and low immune score group (B). Heatmaps of DEGs clustering in immune score group (C) and stromal score group (D), respectively. E, Intersection Venn diagram of significant high expression genes of immune score group and stromal score group. F, Intersection Venn

diagram of significant low expression genes of immune score group and stromal score group. DEGs, differentially expressed genes; AML, acute myeloid leukemia

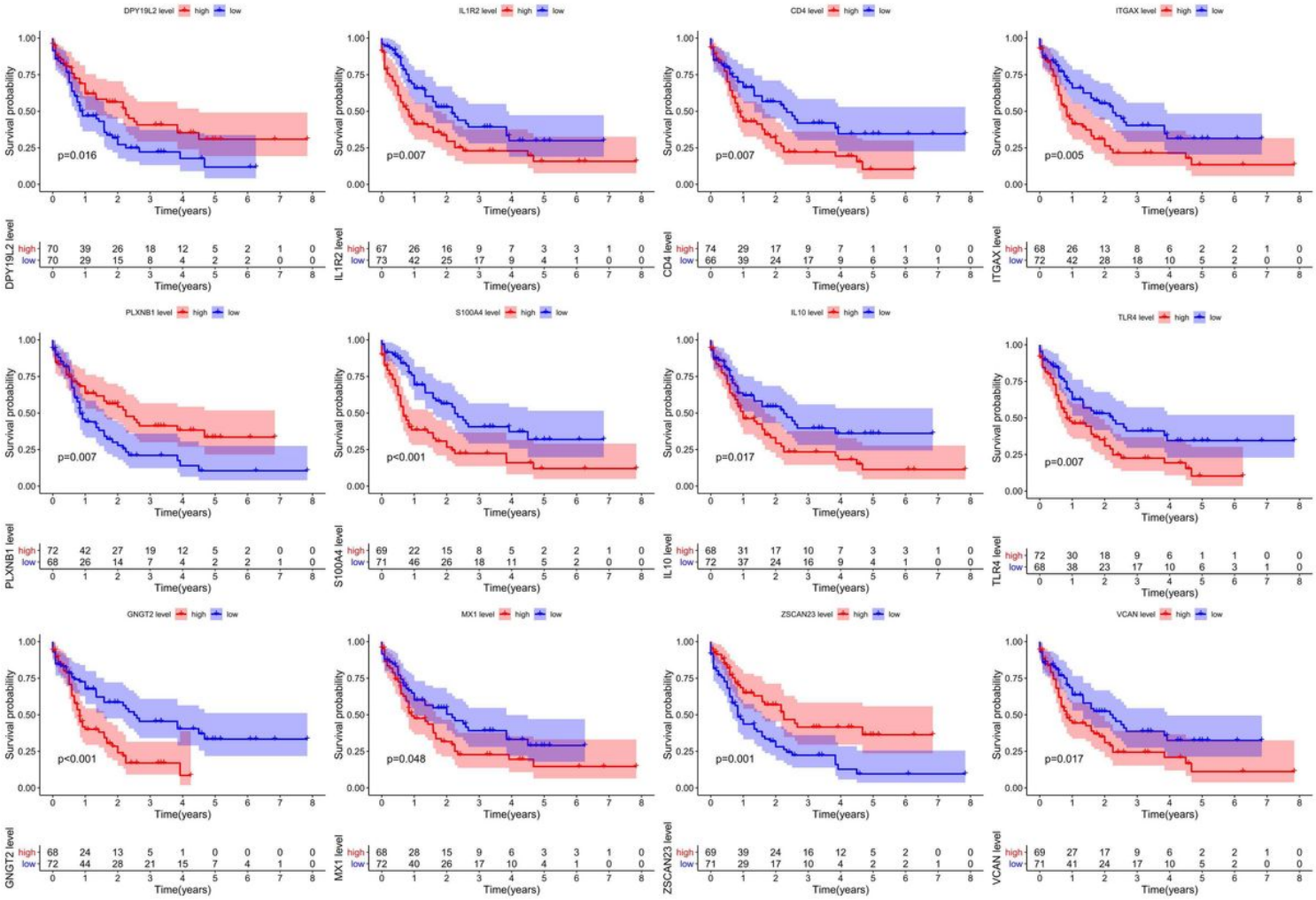

Figure 3

Kaplan–Meier curves of OS for crossed DEGs. DEGs, differentially expressed genes; AML, acute myeloid leukemia; OS, overall survival

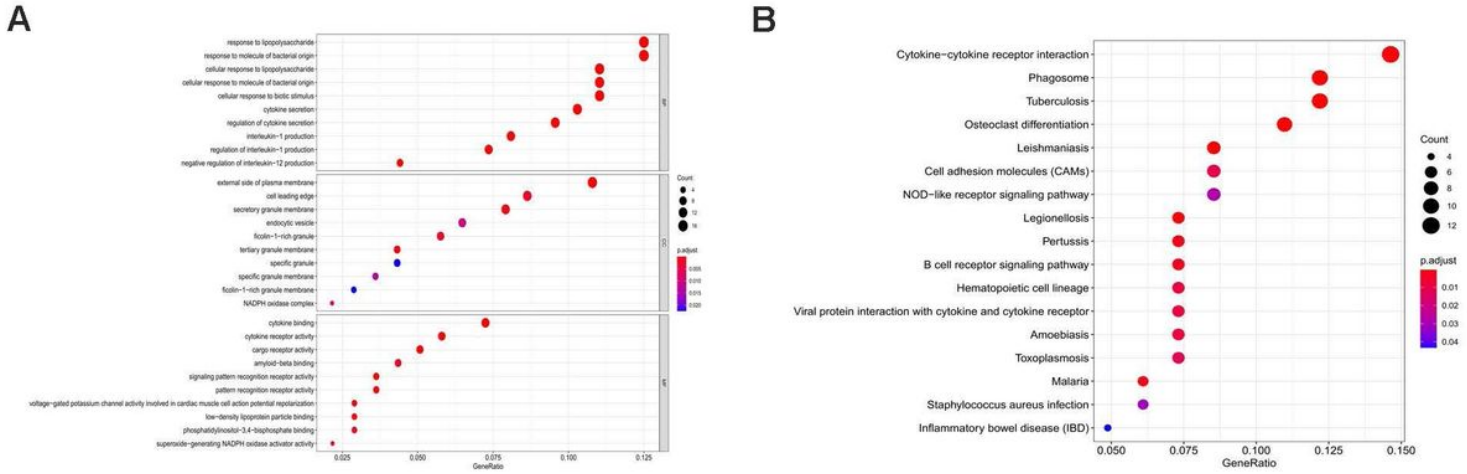

Figure 4

Functional enrichment analysis of crossed DEGs with prognostic indication. A, The results of GO biological process enrichment, cellular component enrichment and molecular function enrichment. B, The result of KEGG pathways analysis of crossed DEGs. DEGs, differentially expressed genes; GO, Gene Ontology; KEGG, Kyoto Encyclopedia of Genes and Genomes

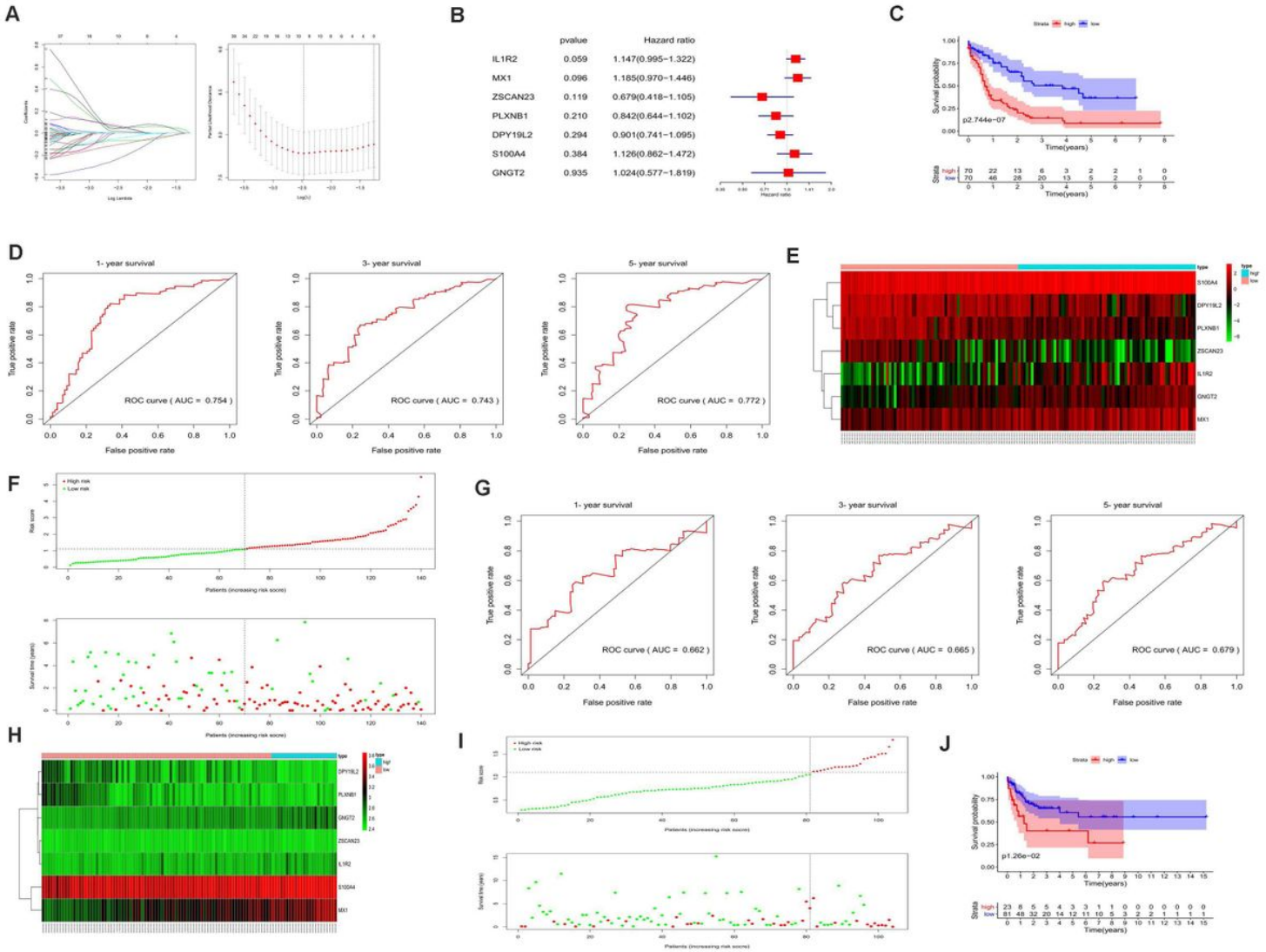

Figure 5

Establishment of a seven-gene signature in the TCGA database and verified with GSE71014 data. A, LASSO coefficient profiles of genes screened from univariate Cox regression analysis (left), The partial likelihood deviance plot selected the best parameters in LASSO model (right). B, Seven genes (IL1R2, MX1,ZSCAN23, PLXNB1 ,DPY19L2,S100A4 and GNGT2) were selected for constructing a gene signature using multivariate Cox regression model. C, Kaplan- Meier survival curves showed the prognostic value of the risk signature between low-risk group and high-risk group in the TCGA database. D, The AUCs of the gene signature for predicting the 1-, 3- and 5-year survival rates in the TCGA database. E, F, The seven genes expression profiles, the risk scores distribution and patients' survival status in the TCGA database. G, The AUCs of the gene signature for predicting the 1-, 3- and 5-year survival rates in the GSE71014 dataset. H, I, The seven genes expression profiles, the risk scores distribution and patients' survival status

in the GSE71014 dataset. J, Kaplan-Meier survival curves showed the prognostic value of the risk signature between low-risk group and high-risk group in the GSE71014 dataset. TME, tumor microenvironment; TCGA, The Cancer Genome Atlas; AUC, the area under curves

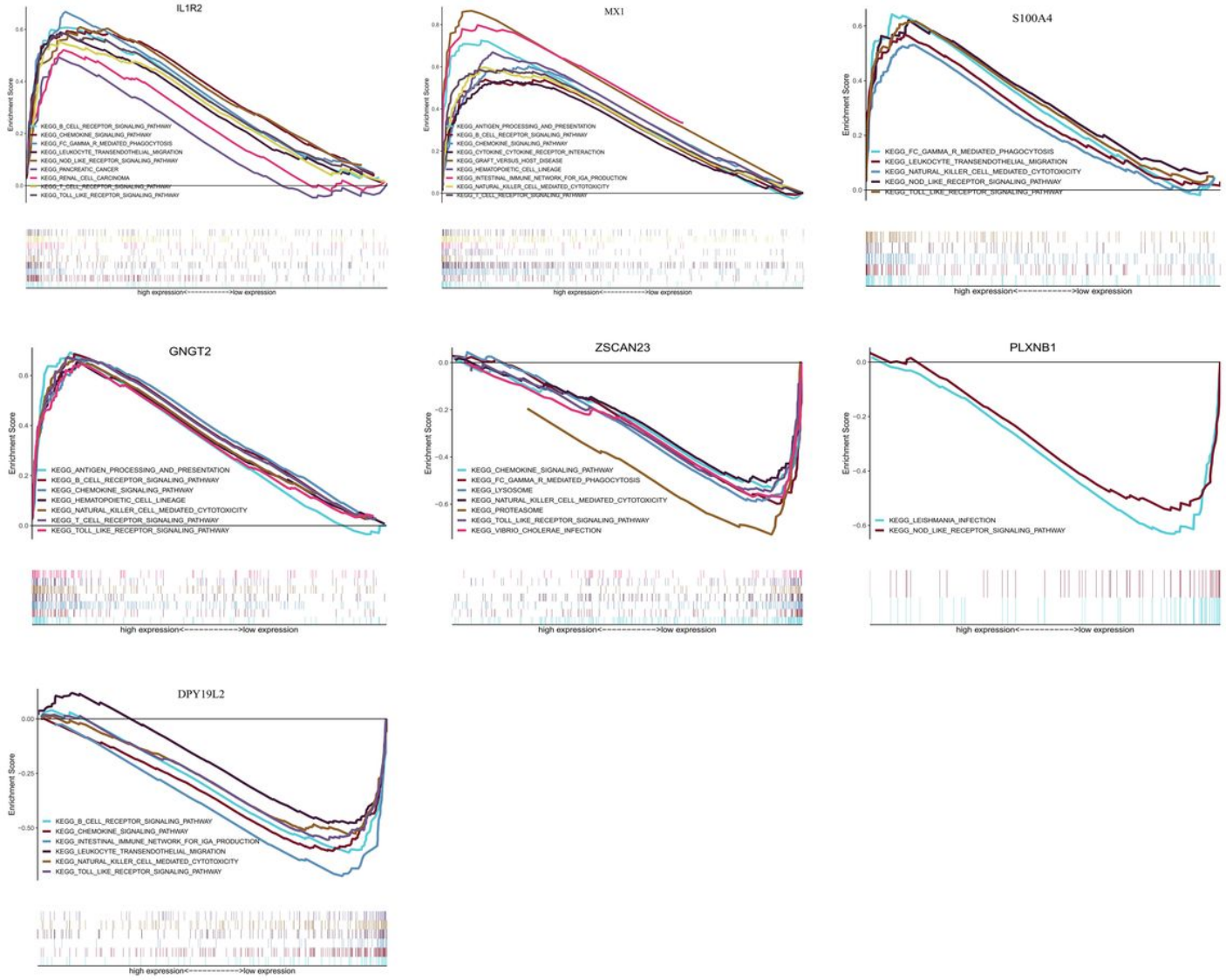

Figure 6

Results of gene set enrichment analysis of genes in the gene signature

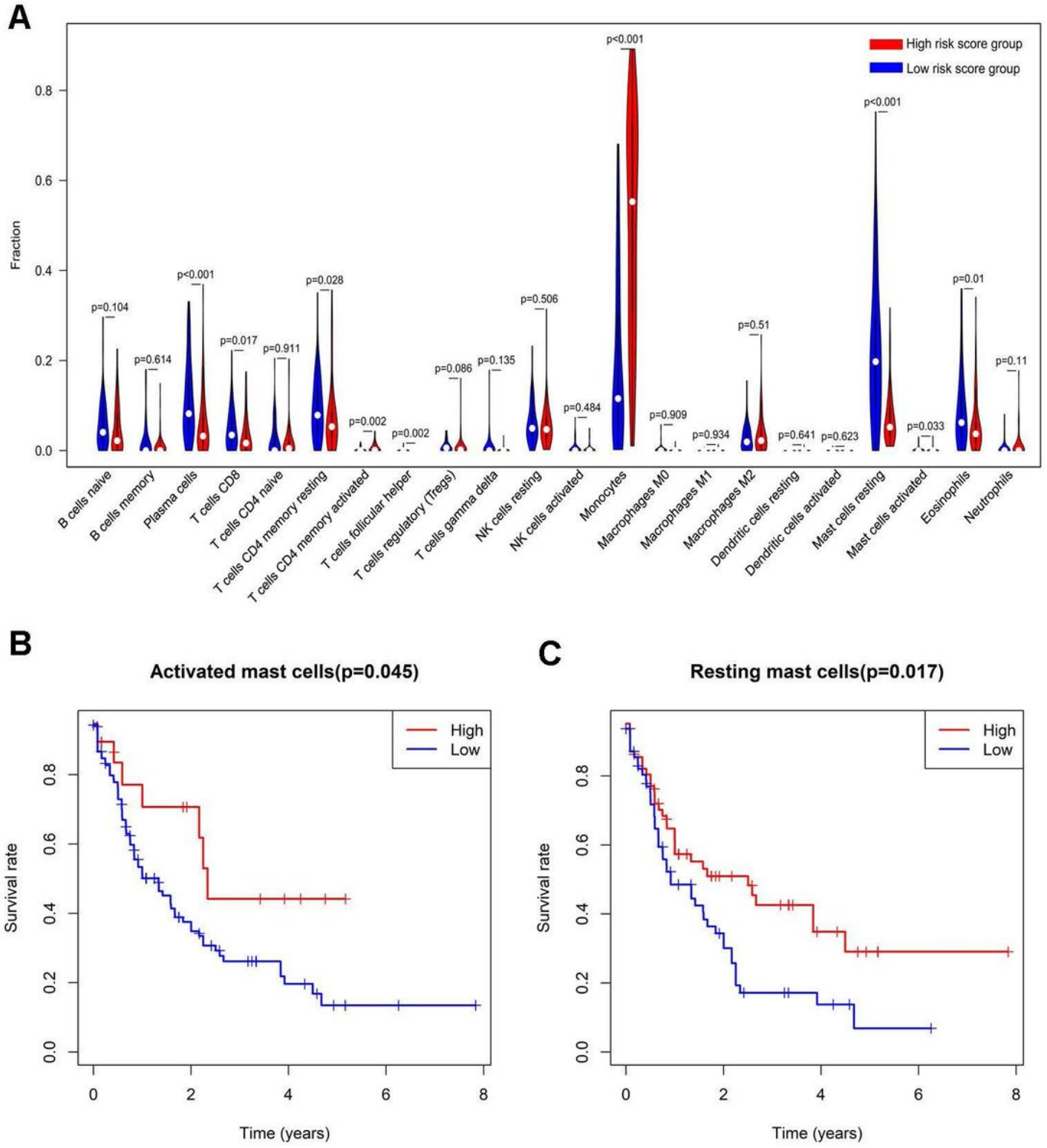

Figure 7

Violin plot of immune infiltration signatures in the high and low risk score groups (A). Kaplan-Meier survival curves showed the prognostic value of activated mast cells(left) and resting mast cells(right) between low proportion and high proportion(B).

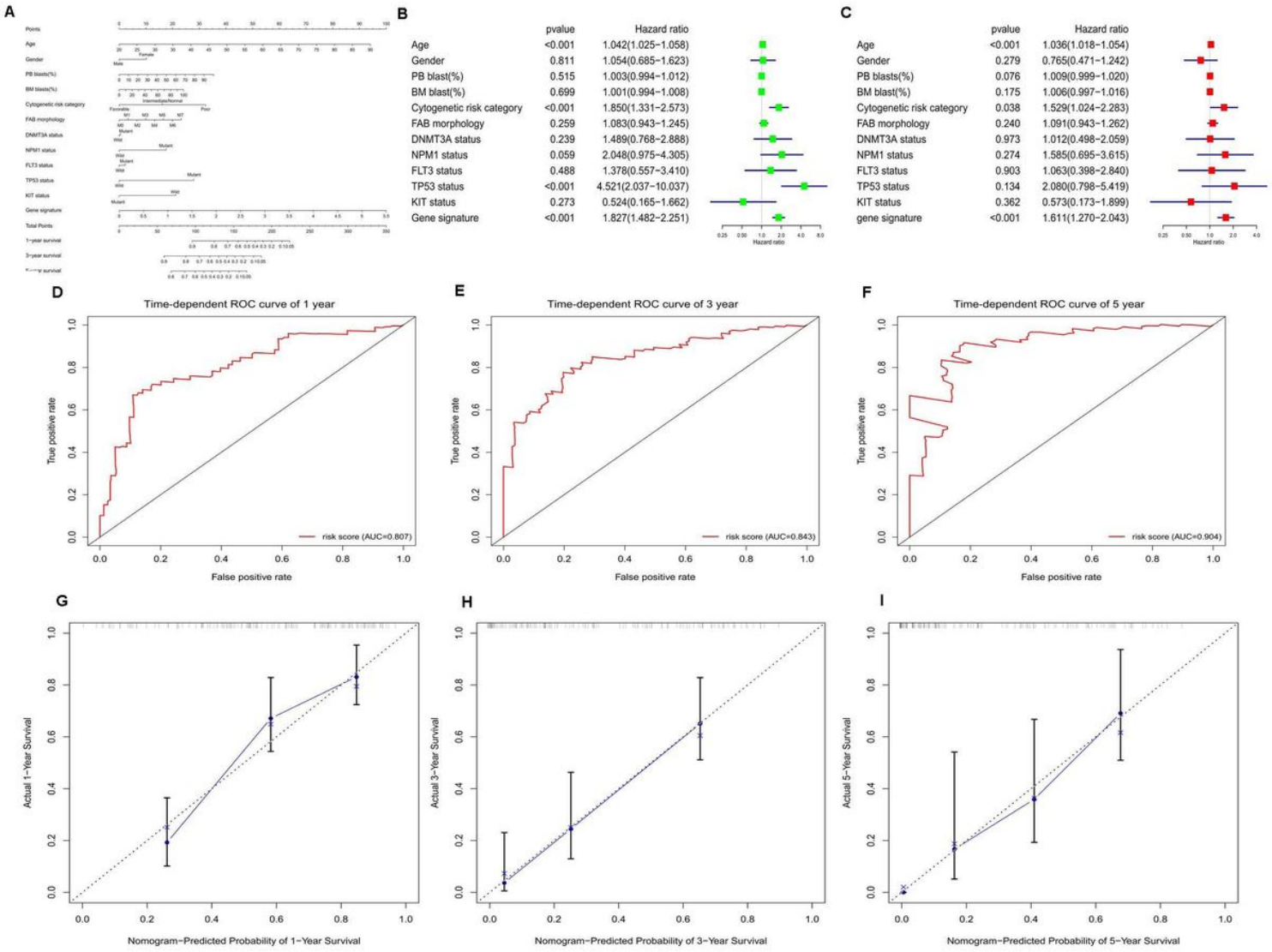

Figure 8

Construction of a nomogram for predicting 1-, 3- and 5-y survival of AML. A, A nomogram for predicting 1-, 3- and 5-y survival rates of AML patients. The univariate(B) and multivariate Cox regression models(C) evaluated the contribution of each variable to AML survival. The AUCs assessed the efficiency of the nomogram for predicting 1- (D), 3- (E) and 5-y (F) survival. Calibration curves showed the probability of 1- (G), 3- (H) and 5-y survival (I) between the prediction and the observation. AML, acute myeloid leukemia; AUC, the area under curves

Supplementary Files

This is a list of supplementary files associated with this preprint. Click to download.

- Table1.docx
- TableS1.xlsx
- TableS2.xls